Progress In Electromagnetics Research C, Vol. 139, 187-195, 2024

PIER C

(Received 26 October 2023, Accepted 5 December 2023, Scheduled 29 December 2023)

Gain Enhanced 26 GHz Antenna for 5G Communication Technology

Eko Setijadi[1,*], Prasetiyono Hari Mukti[1], and Wolfgang Bosch[2]

[1]Department of Electrical Engineering, Sepuluh Nopember Institut of Technology, Indonesia
[2]Department of Electrical Engineering, Graz University of Technology, Austria

ABSTRACT: Wireless technology, a longstanding focus for researchers, has evolved into an exciting telecommunications topic over several decades. The most recent iteration, Fifth Generation (5G), has been introduced at high frequencies, commonly called millimeter waves. An integral component supporting wireless communication is the antenna. This report details the design of a microstrip antenna operating at a frequency of 26 GHz. The antenna is configured as a rectangular patch microstrip, utilizing coupled slot feeding, organized as an array, and implementing a ring as the gain enhancement technique. The designed antenna undergoes observation for both single-element and 1×2 arrays, both with and without rings. A thorough analysis encompasses gain, bandwidth, return loss, and radiation pattern. The antenna design, developed at a frequency of 26 GHz, demonstrates a substantial gain increase of up to 10 dB and 14 dB in the single-element and 1×2 array configurations achieved by adding a ring. The designed antenna surpasses the previous work's gain of about 3 dB more.

1. INTRODUCTION

The telecommunication industry is rapidly advancing wireless technology to meet the escalating demand for faster data transfer speeds and increased bandwidth driven by the proliferation of mobile devices. However, this progress presents challenges regarding limited device performance in transmitting data and multimedia applications with low latency. A specific concern revolves around the allocation of frequency and equipment used in wireless technology applications, where antennas play a pivotal role in supporting various technologies such as Wireless Local Area Network (WLAN), Third Generation (3G), Fourth Generation (4G), and Fifth Generation (5G). With the Internet of Things (IoT) facilitating communication between wireless devices and accommodating vast amounts of data, the necessity for fast and reliable connections has surged exponentially in the past two decades. Despite the anticipation of widespread adoption of 5G by 2025, it has yet to achieve complete standardization, with the 3G Partnership Project (3GPP) 5G Release-16 expected to be adopted by 2022. The upcoming 5G systems promise higher capacity, faster data speeds, low latency, and reliable communication for numerous connected devices. Connectivity trends are shifting, emphasizing low latency, high user densities, enhanced multimedia services, IoT, convergence of applications, and accurate positioning, as reported in [1–5]. While 5G technology offers high data rates, low latency transmission, massive device connectivity, and increased channel capacity, it poses implementation challenges for both Base Transceiver Station (BTS) and User Equipment (UE). This generation of wireless technology utilizes high-frequency millimeter waves to transmit data, leveraging their wider bandwidth compared to 3G and 4G technology, making them more efficient at carrying information. Millimeter waves exhibit tremendous potential, as their band can support data transfer speeds and capacities hundreds of times greater than current cellular capacity.

Designing an antenna for a 5G network requires considering several crucial requirements to ensure the best performance. These prerequisites encompass operating at high frequencies, typically above 24 GHz, to accommodate the elevated frequency bands utilized in 5G. A critical concept underpinning 5G technology involves exploring the untapped spectrum in the high-frequency millimeter wave band (3–300 GHz) [4]. The frequency range between 5.15 GHz and 5.925 GHz resides within the unlicensed band in the sub-6 GHz range. It has been extensively studied in numerous research papers as a promising option for 5G deployment. Furthermore, higher spectrum bands, such as 24.25–27.5 GHz, 26.5–27.5 GHz, 37–37.6 GHz, and 37.5–42.5 GHz, are actively utilized by different countries for 5G implementation [6–8]. The antenna size must be low-profile and compact to facilitate easy integration into various infrastructures, including street lamps, utility poles, and buildings. Simultaneously, it should achieve high efficiency and gain to ensure the required coverage and capacity. In conclusion, achieving optimal performance in the challenging 5G network environment requires meticulous attention to the design of 5G antennas, ensuring they meet the requirements.

Researchers commonly employ microstrip antennas in wireless communication owing to their low profile, lightweight nature, cost-effectiveness, and ease of integration with other microwave components. Nevertheless, their low gain can pose limitations in specific applications. Various techniques are available to enhance the gain of microstrip antennas [9–17]. One approach involves increasing the substrate thickness, redi-

* Corresponding author: Eko Setijadi (setijadieko@gmail.com).

recting the radiation pattern towards the broadside, resulting in higher gain [9]. Another technique employs high dielectric constant substrates, enabling a reduction in antenna size while maintaining the same gain [10]. Additionally, enhancing the patch size, incorporating a parasitic element [11, 12], utilizing an array [13, 14], or employing a feeding technique with higher efficiency can improve the gain of a microstrip antenna [15, 16]. Ghenjeti et al. [17] have proposed a high-gain rectangular microstrip antenna design for 5G broadband applications at the 26 GHz frequency, utilizing an array and contacting inset feed line. The choice of technique depends on specific application requirements, such as frequency range, bandwidth, and size constraints.

This study employed a combined technique involving coupled slot feeding, array elements, and the addition of a ring to a rectangular patch antenna. The aim was to achieve increased gain and expanded bandwidth, aligning with the specified requirements for antennas in 5G technology applications. Designing an antenna that meets specific parameters is crucial for effective operation within the desired frequency range. Microstrip antennas have gained popularity as a viable option for wireless communication due to their compact size and cost-effectiveness in manufacturing. They are well-suited for high-frequency operations and can be easily printed and integrated on the same board as the circuit.

In this report, we developed a single-element and an array microstrip antenna designed to operate at a frequency of 26 GHz with enhanced gain. Adding a ring can enhance the gain for a single element and 1×2 array elements, specifically resulting in a gain of 4.4 dB and 4.5 dB more, respectively. The single element and the 1×2 element array surpass [17] in terms of gain and bandwidth, with specific values of 2.5 dBi, 3.34 GHz, 3.4 dBi, and 1.2 GHz more, respectively.

The paper is organized into five sections. Section 2 details the antenna geometry and the combined technique of coupled slot feeding, array elements, and the addition of a ring to the rectangular patch antenna. The fabrication process of the designed antenna is presented in Section 3. Section 4 focuses on the antenna's performance, including discussions on return loss, gain, bandwidth, and radiation pattern. Finally, Section 5 concludes the present work.

2. ANTENNA DESIGN

Microstrip antenna arrays represent a popular technique employed to enhance the performance of microstrip antennas in terms of gain, directivity, and pattern shaping. Such arrays comprise multiple individual elements, each with its feeding network, arranged in a specific configuration to achieve the desired performance. Utilizing microstrip antenna arrays can yield advantages such as increased gain and reduced size and weight. The constructive combination of radiation from individual elements in microstrip arrays can result in a more directional pattern, leading to significant gain improvements compared to single microstrip antennas. Additionally, microstrip arrays can be more compact and lightweight than conventional antenna arrays based on waveguide or coaxial structures, rendering them an attractive option for various applications. In summary, deploying microstrip antenna arrays provides several benefits over single microstrip antennas, encompassing increased gain, pattern shaping, frequency selectivity, and size and weight reduction. This makes them a popular and versatile choice for various wireless communication, radar, and sensing systems applications.

This investigation aims to evaluate a series of microstrip antenna designs. The designs under examination comprise a single-element antenna without ring, a single-element antenna with ring, a 1×2 array antenna without ring, a 1×2 array antenna with individual rings, and a 1×2 array antenna with a unified ring. Within these four configurations, we conducted a comprehensive analysis that included measurements of gain, bandwidth, return loss, and radiation pattern characteristics for each design.

2.1. Structure of Single Element Antenna

2.1.1. Radiator Patch

The desired antenna specifications include operating at a frequency of 26 GHz with an input impedance at the feeding of 50 Ohms, achieving a minimum gain of 12 dB (according to the International Telecommunication Union — Telecommunication standard sector's reference), and possessing a wide bandwidth of more than 1 GHz. The rectangular microstrip patch antenna is chosen for its simplicity, low-profile shape, and slot feeding to capitalize on bandwidth expansion and gain enhancement. The substrate material used has a dielectric constant of 3.38, with an antenna substrate thickness of 0.813 mm. The feeder width is 0.86 mm. The overall structure comprises three layers: patch layer, ground plane layer, and feedline layer. The designed single-element is depicted in Figs. 1(a)–(e).

Figure 1(a) is a side view of the structure, showing that the antenna consists of a patch layer, a ground plane layer, and a feeding layer, while there is a substrate material between them. The overall thickness of the substrate, h_{total}, is measured from the patch layer to the feeding layer. Fig. 1(b) is the structural geometry of the patch where there is a rectangular patch as a radiator for the antenna configuration without a ring. Fig. 1(c) is the ground plane layer structure containing rectangular slots. Fig. 1(d) is the bottom view structure of the feeding layer on which a feeding line is designed to supply the antenna. Meanwhile, Fig. 1(e) is the top view structure of the patch layer for antenna configuration using a ring.

Several equations about the geometry of the radiator, ground plane, feeding line, and slot structures utilize the approaches introduced by Balanis [18]. A microstrip antenna's typical bandwidth (BW) can be approximated using the equation from [19]. The theoretical view of fractional bandwidth is defined as the ratio of bandwidth to the resonant frequency

$$\mathrm{BW}[\%] = \frac{f_u - f_l}{f_r} \times 100\%, \tag{1}$$

where f_u and f_l represent the upper and lower frequencies of the antenna, respectively, taken from the region where $S_{11} < -10$ dB.

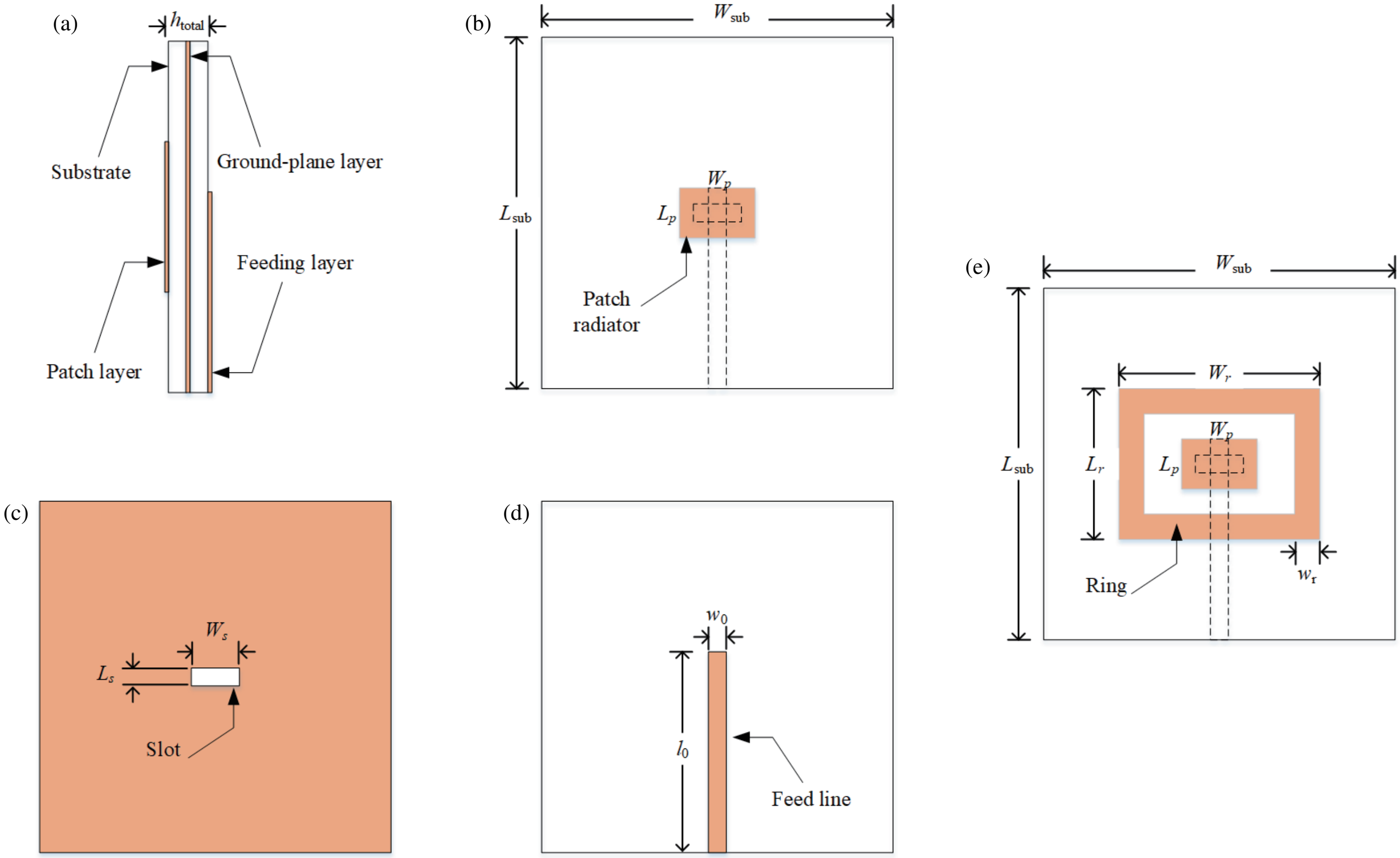

FIGURE 1. Antenna structure with and without adding ring (a) side view, (b) top view without added ring, (c) slot on the ground plane, (d) bottom view, and (e) top view with added ring.

2.1.2. Feeding Technique

Antenna designers widely employ the coupled slot feeding technique to feed microstrip antennas by coupling the microstrip patch through a slot on the ground plane. This technique offers several advantages over other feeding methods, including enhanced bandwidth due to the additional degree of freedom the slot provides for tuning the resonant frequency and achieving a broader impedance bandwidth. Moreover, it reduces insertion loss by providing a more efficient means of coupling energy from the feed line to the antenna. The coupled slot feeding technique also yields compact, low-profile antennas with polarization flexibility. It seamlessly integrates with other microwave components, such as filters, couplers, and amplifiers, making it a popular choice for antenna designers.

The following equation approximates the characteristic impedance of a strip feeding with width w_0 under the condition $w_0/h > 1$.

$$Z_{\text{char}} = \frac{120\pi}{\sqrt{\varepsilon_{\text{eff}}}\left[\frac{w_0}{h} + 1.393 + 0.667\ln\left(\frac{w_0}{h} + 1.444\right)\right]}. \quad (2)$$

For a slot in a rectangular form with dimensions L_s and W_s, optimum directivity is achieved within the sector angle $(0 \leq \theta \leq \theta_{EH})$ for both E-plane and H-plane. The following equation expresses the optimum angular angle for the E-plane in coupled slot feeding.

$$L_s = \frac{\lambda}{\sin\theta_E}, \quad (3)$$

and H-plane

$$W_s = \frac{\lambda}{\sin\theta_H}. \quad (4)$$

2.1.3. Associated Parameters

The following equation expresses the return loss, which indicates the power loss returned from the load towards the source due to impedance mismatch [20].

$$\text{RL} = -\text{S}_{11}\ [\text{dB}], \quad (5)$$

where S_{11} is equal to reflected coefficient Γ that is represents a ratio between incidence and reflected wave

$$\text{S}_{11} = \Gamma = \frac{b_1}{a_1}, \quad (6)$$

TABLE 1. Geometry of the antenna elements with and without added ring.

L_p [mm]	W_p [mm]	L_s [mm]	W_s [mm]	L_{sub} [mm]	W_{sub} [mm]	l_0 [mm]	w_0 [mm]	$L_r w_r$ [mm]	W_r [mm]	w_r [mm]	h_{total} [mm]
2	3.3	0.3	2.4	25	25	2	13.4	2	12	16	1.626

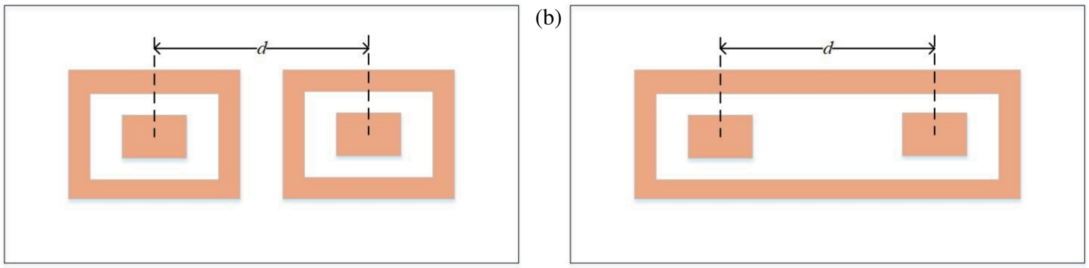

FIGURE 2. Structure of 1×2 array antenna. (a) Array with independent rings. (b) Array with a unify ring.

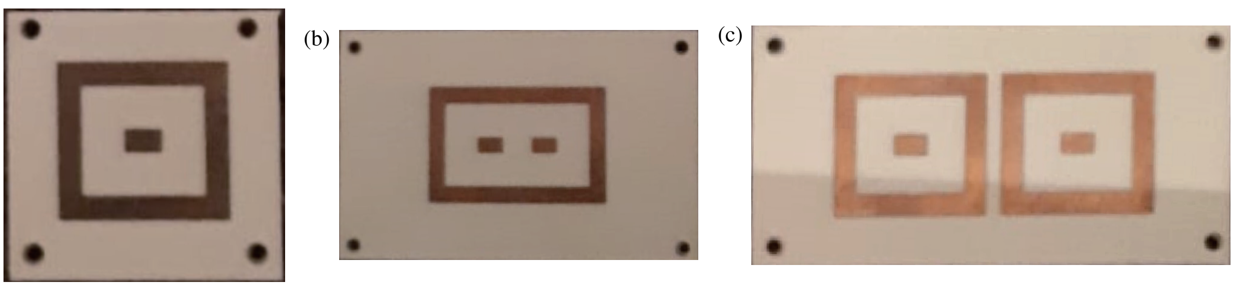

FIGURE 3. Fabricated antenna with applied ring. (a) Single element with a ring. (b) 1×2 array with a ring. (c) 1×2 array with independet rings.

where a_1 and b_1 are incidence and reflected wave, respectively.

$$\mathrm{S}_{11}\ [\mathrm{dB}] = 20\log_{10}(|\Gamma|). \tag{7}$$

Table 1 provides the initial geometry of the designed antenna structures and is linked to Figure 1. The parameters L_p, W_p, L_s, W_s, L_{sub}, L_{sub}, l_0, w_0, L_r, W_r, and w_r represent the patch length, patch width, slot length, slot width, substrate length, substrate width, feedline length, feedline width, ring length, ring width, and ring thickness, respectively. The size of the ground plane is identical to the size of the substrate. The term h_{total} denotes the substrate thickness from the ground plane to the patch radiator.

2.2. Structure of 1 x 2 Array Antenna

Figure 2 illustrates the structure of a 1×2 antenna array composed of a single-element structure that has been designed. In Fig. 2(a), the array structure is added independently to each element, and in Fig. 2(b), a ring is added that unifies the elements. The distance between adjacent elements will be varied between $1/2\lambda$ and λ to evaluate the optimal space for the designed array.

3. ANTENNA FABRICATION

The fabricated antennas were measured using a Vector Network Analyzer (VNA) to investigate S_{11} and radiation patterns. Furthermore, parameters such as return loss, bandwidth, Half Power Bandwidth (HPBW), gain, and side lobe were deeply investigated to extract the performance of the designed antenna. The antenna was made using Rogers RO4003C and etched according to the structures shown in Figs. 1 and 2 with dimensional parameters in Table 1. The fabricated antenna scenarios include a single element without and with a ring, a 1×2 array without and with ring, and a 1×2 array with independent rings. Some of the fabricated antennas are shown in Fig. 3(a) Single antenna with a ring, (b) 1×2 array with ring, and (c) 1×2 array with independent rings.

4. PERFORMANCE OF THE ANTENNA AND DISUSSION

4.1. Single Element with and without Ring

Figure 4 depicts the correlation between the substrate thickness and bandwidth of the microstrip patch antenna, as outlined in the equation in [19]. A thicker substrate yields a broader band-

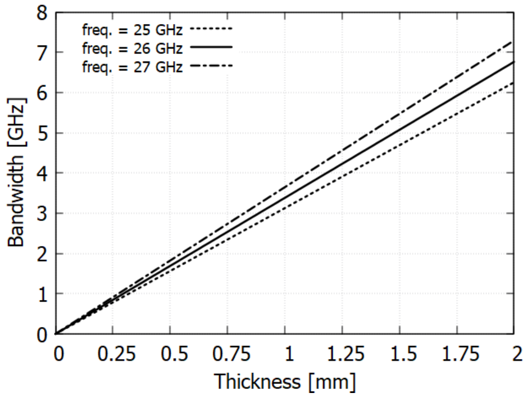

FIGURE 4. Bandwidth vs thickness.

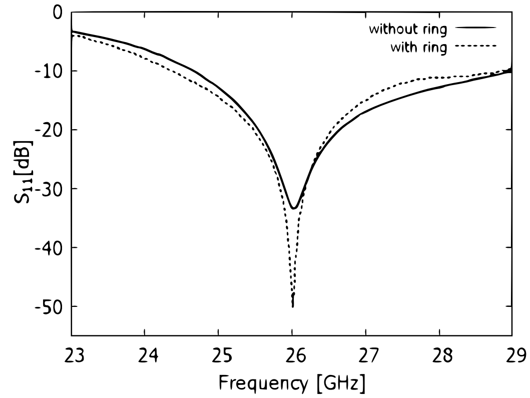

FIGURE 5. S_{11} of the single element antenna with and without ring.

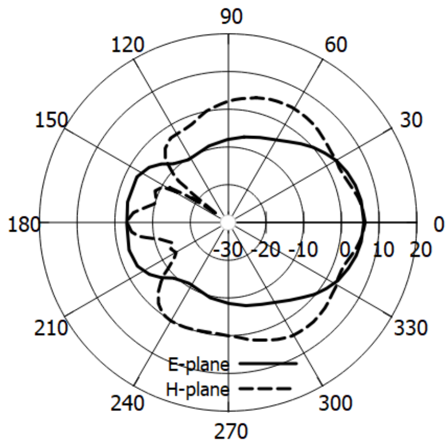

FIGURE 6. E-H plane radiation pattern of with and without a ring.

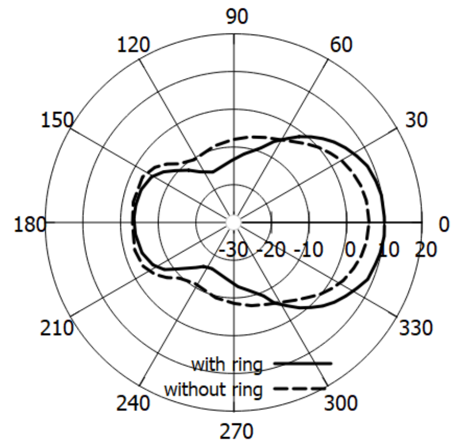

FIGURE 7. E-plane radiation pattern of with and without a ring.

width; this phenomenon occurs dominantly at higher frequencies, which play a role in expanding the bandwidth of the microstrip antenna. In the designed antenna, the overall thickness of the substrate between the feeding and the radiator h_{total} is 1.626 mm, operating at 26 GHz, resulting in a bandwidth equivalent to 5.5 GHz.

Figure 5 elucidates the return loss characteristics of a single-element antenna, both with and without a ring. The single element equipped with ring demonstrates a notably superior return loss of 48 dB compared to the configuration without ring, which records 33.3 dB. Notably, in both scenarios of the single antenna, the expansive bandwidth is evident through the observation of return loss values, each measuring higher than or equal to 10 dB or, equivalently, with forward power exceeding 90%. The figure shows frequency ranges of 24.35–28.97 GHz and 24.6–29 GHz for the single-element antenna with and without ring, respectively.

Figure 6 depicts the radiation pattern of a single antenna element in the E-plane and H-plane. The maximum level at the boreside direction of 0° in both E-plane and H-plane gives a gain of 6 dB. Each exhibits a beamwidth of 90° and 80° for the E and H planes, respectively. Only a back lobe is present in the E-plane, while side and back lobes are evident in the H-plane. The minimal side lobe level in the H-plane requires consideration for communication or radar systems applications, which generally demand a low side lobe level. The beamwidth aligns with the expressions in Eqs. (3) and (4) utilized in designing the size of the slot of the feeding coupler.

Figure 7 compares the E-plane radiation patterns of single-element antennas with and without a ring. Both antennas exhibit maximum gain at an angle of 0°, measuring 6 dB and 10.4 dB, respectively. The antenna with ring shows a gain increase of more than 4 dB compared to the antenna without ring. This gain enhancement results from the altered beamwidth of the antenna when the ring is used, which measures 72° and 66° without and with ring, respectively. Adding ring to the antenna's radiator reduces the beamwidth, effectively enhancing the directivity and, consequently, the gain proportionally.

The H-plane exhibits similar behaviour to what occurs in the E-plane. There is an increase in gain of more than 4 dB with a smaller beamwidth, decreasing from 48° to 30° in the antenna with ring compared to the antenna without ring. This is illustrated in Figure 8. The H-plane exhibits a smaller beamwidth than the E-plane due to the geometry of L_s being smaller than W_s, as well as the size of the ring where the geometry parallel to the E-plane is smaller than the geometry of the ring parallel to the H-plane.

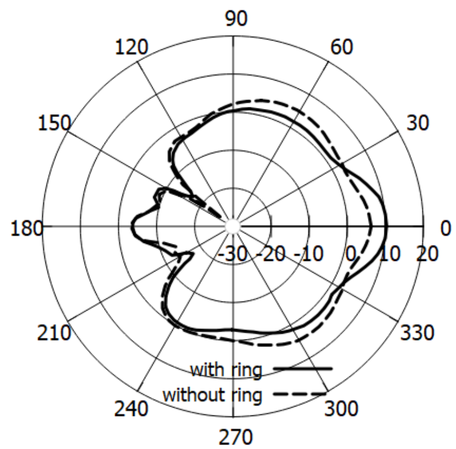

FIGURE 8. H plane radiation pattern of with and without ring.

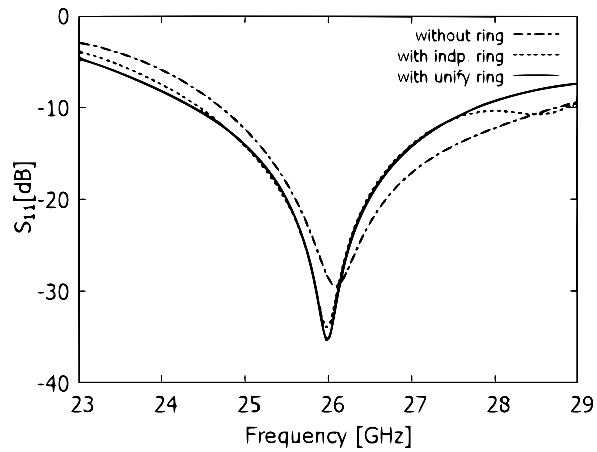

FIGURE 9. S_{11} of array antenna without ring, with independent rings, and with a unify ring.

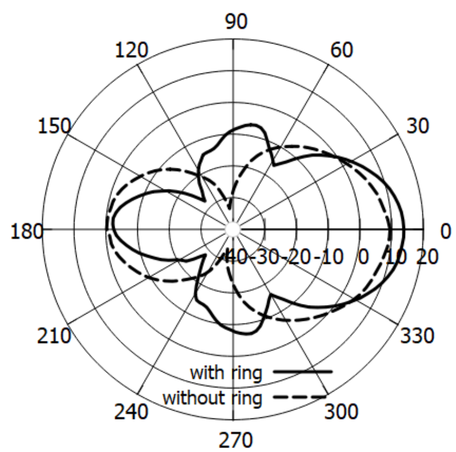

FIGURE 10. Radiation pattern of array antenna $d = 1/2\lambda$.

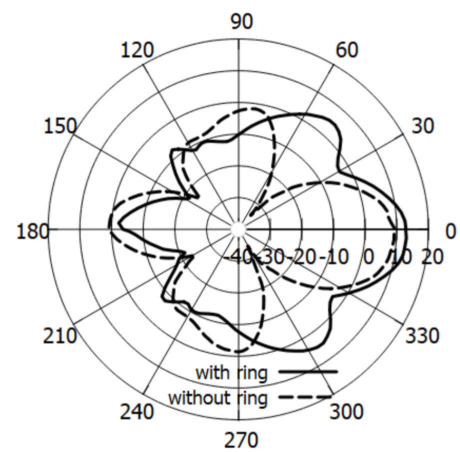

FIGURE 11. Radiation pattern of array antenna $d = \lambda$.

4.2. 1 x 2 Elements Array with and without Ring

The return loss performance, as depicted in Fig. 9, is compared for configurations without and with a ring. The return loss of the antenna with ring shows a significantly smaller value than that without ring. Meanwhile, the antenna's return loss using independent and unified rings exhibits a slight difference. This implies that the antenna's gain with ring is significantly greater than that without ring. Analyzing the S_{11} by considering return loss and bandwidth, it is observed that without a ring and with a ring, the antenna provides bandwidth in the range of 24.75–28.7 GHz and 24.4–27.7 GHz, with return loss values of 28 dB and 35 dB, respectively. Applying independent and unified rings to the antenna array radiator contributes to an increase in return loss of up to 7 dB compared to the array antenna without rings.

The radiation patterns of the 1×2 array antenna with ring for space between elements $d = 1/2\lambda$ are shown in Fig. 10. The gain of the antenna with ring is 14 dB, while without ring, it is 9.5 dB, an increasing gain of 4.5 dB. The HPBWs of the 1×2 array antenna with and without ring are 31.5° and 36°, respectively. The side lobe provided by the 1×2 array antenna with ring is -6.8 dB at 80° and -6.4 dB at 77°. Notably, there is no side lobe for the 1×2 array antenna without ring.

Figure 11 depicts the radiation pattern of a 1×2 array antenna with space $d = \lambda$ for those with and without ring. The gain with a ring is 12 dB, while without ring, it is 9 dB, increasing the gain of 3 dB. The HPBWs of the 1×2 array antenna with and without ring are 345.2°–8.8° and 342.8°–9.2°, respectively. The side lobe provided by the 1×2 array antenna with ring is 4.8 dB at 307° and 4.84 dB at 47.15°, while the 1×2 array antenna without ring provides side lobe of -1.37 dB at 270.2° and -1.6 dB at 81.8°.

Figure 12 illustrates the radiation pattern of a 1×2 array antenna without ring for space $d = 1/2\lambda$ and $d = \lambda$ configurations. In both configurations, the gain in the boreside direction reaches the same value at 9.5 dB. At a space of $d = \lambda$, side lobes appear at the -2 dB level at 270.2° and 81.8° directions, while there is no side lobe at $d = 1/2\lambda$. Despite the smaller beamwidth, the gain does not increase due to the emergence of side lobes in the configuration with space at $d = \lambda$.

Figure 13 illustrates the radiation pattern of the antenna array for different distances using a ring. The gain achieved in the

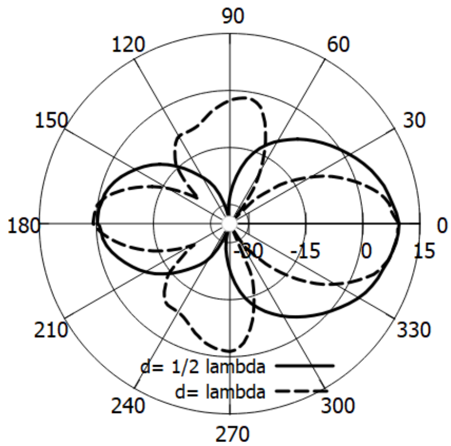

FIGURE 12. Radiation pattern of array antenna without using ring for $1/2\lambda$ and λ.

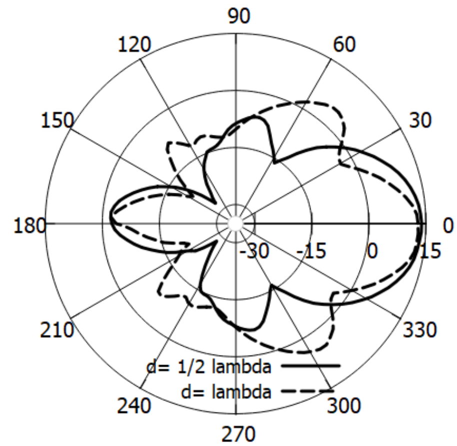

FIGURE 13. Radiation pattern of array antenna with using ring for $d = 1/2\lambda$ and $d = \lambda$.

TABLE 2. Comparison of the antenna design scenarios.

Parameter	**Single element**		**Array 1×2 elements**	
	Without a ring	**With a ring**	**Without a ring**	**With a ring**
Return loss	33 dB	48 dB	28 dB	35 dB
Bandwidth	4.4 GHz [24.6–29 GHz]	4.62 GHz [24.35–28.97 GHz]	3.95 GHz [24.75–28.7 GHz]	3.3 GHz [24.4–27.7 GHz]
Gain	6 dB	10.4 dB	$[d = 1/2\lambda]$ 9.5 dB $[d = \lambda]$ 9 dB	$[d = 1/2\lambda]$ 14 dB $[d = \lambda]$ 12 dB
HPBW	72°	66°	$[d = 1/2\lambda]$ 36° $[d = \lambda]$ 18°	$[d = 1/2\lambda]$ 31° $[d = \lambda]$ 6°
Side lobe	- -	- -	$[d = 1/2\lambda]$ 2 lobes $[d = \lambda]$ 2 lobes	- $[d = \lambda]$ 4 lobes

boreside direction varies between the 1×2 array with space $d = 1/2\lambda$ and $d = \lambda$ configurations, measuring 14 dB and 12 dB, respectively. At an adjacent distance $d = \lambda$, four side lobes are observed, while for space $d = 1/2\lambda$, there are two lobes. This results in the gain at the adjacent distance $d = \lambda$ being smaller than at $d = 1/2\lambda$. The presence of two prominent side lobes diminishes the gain at the $d = \lambda$ configuration compared to the other.

4.3. Comparison Results

Table 2 compares antenna performances from 4 scenarios: single element with and without ring, 1×2 array with and without ring. Return loss on a single element is more significant than 1×2 array elements with and without ring. Still, both show that adding a ring can increase return loss on a single element and 1×2 array elements, increasing 15 dB and 7 dB, respectively. A single element provides a broader bandwidth than a 1×2 array while adding a ring does not always widen the bandwidth. The gain on a 1×2 array elements is more significant than that of a single element. Adding a ring can increase the gain on a single element or 1×2 array elements, namely 4.4 dB and 4.5 dB, respectively. The HPBW of a single element shows a broader beam than a 1×2 array, and adding a ring can narrow the HPBW to 6 and 5, respectively. Meanwhile, in a 1×2 array, widening the space between elements from $d = 1/2\lambda$ to $d = \lambda$ can reduce the gain. Although the width of the beam narrows at the farther adjacent elements, this increases the number or levels of side lobes.

Table 3 introduces a comparison with the results of previous work [17], which uses the same type as the present work, the Rectangular Microstrip Antenna (RMSA) type. The earlier study aimed to fulfil the same objective as the proposed antenna design, specifically meeting 5G application specifications at the 26 GHz frequency. The proposed antenna design exhibits a higher return loss for both the single patch and the array with two elements (1×2), indicating more tremendous emitted energy. Additionally, the proposed design demonstrates higher gain with a broader bandwidth than the previous work. On a single element, it achieves higher return loss, higher gain, and broader bandwidth than [17], a single element of 21.92 dB,

TABLE 3. Comparison with other work results.

Reference	Frequency [GHz]	Antenna type	Number of elements	Return Loss [dB]	Gain [dBi]	BW [GHz]
[17]	26	RMSA	1	26.08	7.9	1.28
	26	RMSA	2	21.92	11	2.1
Proposed design	26	RMSA	1	48	10.4	4.62
	26	RMSA	2	35	14.4	3.3

2.5 dB, and 3.34 GHz, respectively. Likewise, the 1×2 element array has a higher return loss, higher gain, and broader bandwidth than in the case of [17], respectively.

5. CONCLUSION

An antenna featuring a single-element and a 1×2 array configuration has been presented for operation at a frequency of 26 GHz. This achievement is realized by incorporating a ring structure, resulting in enhanced gains of up to 10 dB and 14 dB for the respective configurations. The antenna is constructed by combining a rectangular patch radiator, coupled slot feeding, and applying a ring structure. Employing the slot technique in the supply system is highly suitable for high frequencies due to the tiny size of the radiator. Additionally, this feeding technique offers the advantage of significantly increased gain compared to conventional methods. Adding a ring structure around the radiator narrows the HPBW and increases the gain. Designing arrays with proper spacing further contributes to gain enhancement. A single element without a ring exhibits a gain of 4 dB. In comparison, introducing a ring to the single element increases the gain to 10 dB, marking a gain augmentation of approximately 6 dB. An unringed 1×2 array with an adjacent distance of $d = 1/2\lambda$ achieves a gain of 10 dB, while a 1×2 array with a ring and the same space $d = 1/2\lambda$ attains antenna's gain of 14 dB. The design of adding a ring into the 1×2 array with $d = 1/2\lambda$ spacing results in a gain increase of 4 dB. This design is a reference for future development, particularly for 5G applications. The single element and the 1×2 elements array perform better than the previous works regarding gain and bandwidth, with specific values of 2.5 dBi, 3.34 GHz, 3.4 dBi, 1.2 GHz more, respectively.

ACKNOWLEDGEMENT

The research is funded by an Institut Teknologi Sepuluh Nopember Research Grant for Study Center Collaboration with contract No. 1187/PKS/ITS/2021. We want to thank Prof. Wolgang Bosch, the Graz University of Technology, as a research partner.

REFERENCES

[1] Support 5G, *ITU News Magazine*, 21–23, Nov. 2019.

[2] Andrews, J. G., S. Buzzi, W. Choi, S. V. Hanly, A. Lozano, A. C. K. Soong, and J. C. Zhang, "What will 5G be?" *IEEE Journal on Selected Areas in Communications*, Vol. 32, No. 6, 1065–1082, Jun. 2014.

[3] Agiwal, M., A. Roy, and N. Saxena, "Next generation 5G wireless networks: A comprehensive survey," *IEEE Communications Surveys and Tutorials*, Vol. 18, No. 3, 1617–1655, 2016.

[4] International Telecommunication Union, "Additional frequency bands identified to," Jun. 2014.

[5] Series, M., "IMT vision-framework and overall objectives of the future development of IMT for 2020 and beyond," *Recommendation ITU*, Vol. 2083-0, 2015.

[6] Thakur, V., N. Jaglan, and S. D. Gupta, "A review on antenna design for 5G applications," in *2020 6th International Conference on Signal Processing and Communication (ICSC)*, 266–271, Noida, India, 2020.

[7] Intelligence, G. S. M. A., "Understanding 5G: perspectives on future technological advancements in mobile," *White Paper*, 1–26, 2014.

[8] Chen, S. and J. Zhao, "The requirements, challenges, and technologies for 5G of terrestrial mobile telecommunication," *IEEE Communications Magazine*, Vol. 52, No. 5, 36–43, May 2014.

[9] Dwivedi, S., "Effect of thickness of substrate on antenna design for advance communication," in *Proceedings of The 7th International Conference on Cloud Computing, Data Science and Engineering (Confluence 2017)*, 770–774, Noida, India, Jan. 2017.

[10] Kedze, K. E., H. Wang, Y. B. Park, and I. Park, "Substrate dielectric constant effects on the performances of a metasurface-based circularly polarized microstrip patch antenna," *International Journal of Antennas and Propagation*, Vol. 2022, Sep. 2022.

[11] Pratiwi, A. R., E. Setijadi, and G. Hendrantoro, "Design of two-elements subarray with parasitic patch for 5G application," in *2020 International Seminar on Intelligent Technology and Its Applications (ISITIA)*, 311–316, 2020.

[12] Amillia, F., E. Setijadi, and G. Hendrantoro, "The effect of parasitic patches addition on bandwidth enhancement and mutual coupling in 2 x 2 sub-arrays," *IEEE Access*, Vol. 10, 72 057–72 064, 2022.

[13] Srivastava, H., A. Singh, A. Rajeev, and U. Tiwari, "Bandwidth and gain enhancement of rectangular microstrip patch antenna (RMPA) using slotted array technique," *Wireless Personal Communications*, Vol. 114, No. 1, 699–709, Sep. 2020.

[14] Faeghi, P., C. Ghobadi, J. Nourinia, and B. Virdee, "Nanoparticle-coated vivaldi antenna array for gain enhancement," *Applied Physics A-materials Science & Processing*, Vol. 129, No. 3, Mar. 2023.

[15] Koul, S. K. and G. S. Karthikeya, "Feeding techniques for mmwave antennas," *Antenna Architectures for Future Wireless Devices*, 207–229, 2021.

[16] Ulfah, M. M., P. Janpugdee, and D. Torrungrueng, "Feeding effects to gain enhancement of microstrip antennas with partially reflective surfaces," in *2022 International Symposium on Antennas and Propagation (ISAP)*, 435–436, Sydney, Australia, Oct. 2022.

[17] Ghenjeti, S., R. Barrak, and S. Hamouda, "High gain and compact microstrip patch antenna array design for 26 GHz broadband wireless systems," in *2023 IEEE Symposium on Computers and Communications (ISCC)*, 932–937, 2023.

[18] Balanis, C. A., *Antenna Theory: Analysis and Design*, 4th ed., John Wiley & Sons, Hoboken, New Jersey, 2016.

[19] Johnson, R. C., *Antenna Engineering Handbook*, 3rd ed., McGraw-Hill, New York, 1993.

[20] Huang, Y., *Antennas: From Theory to Practice*, John Wiley & Sons, Singapore, 2008.